Earth and Planetary Science Letters 302 (2011) 448–454

Contents lists available at ScienceDirect

Earth and Planetary Science Letters

journal homepage: www.elsevier.com/locate/epsl

Mantle plumes and associated flow beneath Arabia and East Africa

Sung-Joon Chang *, Suzan Van der Lee

Department of Earth and Planetary Sciences, Northwestern University, 1850 Campus Drive, Evanston, IL 60208-2150, USA

ARTICLE INFO

Article history:
Received 29 April 2010
Received in revised form 25 December 2010
Accepted 28 December 2010
Available online 19 January 2011

Editor: R.W. Carlson

Keywords:
seismic tomography
joint inversion
mantle plume
mantle flow
Arabia
East Africa

ABSTRACT

We investigate mantle plumes and associated flow beneath the lithosphere by imaging the three-dimensional *S*-velocity structure beneath Arabia and East Africa. This image shows elongated vertical and horizontal low-velocity anomalies down to at least mid mantle depths. This three-dimensional *S*-velocity model is obtained through the joint inversion of teleseismic *S*- and *SKS*-arrival times, regional *S*- and Rayleigh waveform fits, fundamental-mode Rayleigh-wave group velocities, and independent Moho constraints from receiver functions, reflection/refraction profiles, and gravity measurements. In the resolved parts of our *S*-velocity model we find that the Afar plume is distinctly separate from the Kenya plume, showing the Afar plume's origin in the lower mantle beneath southwestern Arabia. We identify another quasi-vertical low-velocity anomaly beneath Jordan and northern Arabia which extends into the lower mantle and may be related to volcanism in Jordan, northern Arabia, and possibly southern Turkey. Comparing locations of mantle plumes from the joint inversion with fast axes of shear-wave splitting, we confirm horizontal mantle flow radially away from Afar. Low-velocity channels in our model support southwestward flow beneath Ethiopia, eastward flow beneath the Gulf of Aden, but not northwestwards beneath the entire Red Sea. Instead, northward mantle flow from Afar appears to be channeled beneath Arabia.

1. Introduction

The voluminous Ethiopian flood basalts, widespread Cenozoic volcanism in western Arabia, and anomalous topographic swells have long been attributed to mantle plumes (Camp and Roobol, 1992; Daradich et al., 2003; Ebinger and Sleep, 1998; Schilling, 1973; White and McKenzie, 1989).

Although this region (Fig. 1) has been well studied, there has been no consensus on the number of plumes and associated mantle flow beneath East Africa and Arabia. Ebinger and Sleep (1998) proposed that a single large plume may have caused multiple hotspots via channeled flow along thin lithosphere. This hypothesis has been supported by a number of geophysicists. For example, Ritsema et al. (1999) attribute the extensive volcanism around Afar to mantle flow from the African superplume, which originates at the core–mantle boundary (CMB) beneath South Africa in their global *S*-velocity model. The regional travel time tomographic results of Benoit et al. (2006a,b) support a single plume beneath Ethiopia. Numerical experiments by Daradich et al. (2003) suggest that rift-flank uplift along the Red Sea was induced by the African superplume. On the other hand, numerical mantle convection models of Lin et al. (2005) show that double-plume models can reproduce the distribution of East-African magmatism in space and time. Finite-frequency tomography (Montelli et al., 2004) shows that the Afar plume has a cylindrical, vertical tail through the lower mantle, separate from the African superplume. However, they do not rule out that the Afar plume may merge into the African superplume in the deep lower mantle (Montelli et al., 2006). Shear-wave splitting and tomographic results of Hansen et al. (2006) and Park et al. (2007, 2008) suggest channeled horizontal mantle flow from the Afar hotspot.

On the other hand, several geochemists have proposed the existence of two distinct mantle plumes beneath East Africa. George et al. (1998) used $^{40}Ar/^{39}Ar$ ages to propose distinct mantle plumes beneath Afar and Kenya. Nelson et al. (2007, 2008) and Rogers et al. (2000) also assert two distinct mantle plumes based on Sr, Nd, and Pb isotope evidence. Pik et al. (2006) used He^3/He^4 ratios to suggest that a unique large mantle plume could not feed all the Cenozoic African volcanic provinces. Camp and Roobol (1992) question whether one Afar plume can feed widespread volcanism in western Arabia over a distance of 2000 km, which is twice the radius of a typical plume head (White and McKenzie, 1989). On the contrary, Furman et al. (2006) present geochemical evidence that suggests these different plumes could all stem from a common large mantle plume such as the African superplume.

In summary, current evidence is inconclusive with respect to the following questions. How many mantle plumes exist with different origins beneath East Africa and Arabia? If hot materials are upwelling via those plumes, do they flow along thin lithosphere as a natural

* Corresponding author.
E-mail address: sjchang@earth.northwestern.edu (S.-J. Chang).

0012-821X/$ – see front matter
doi:10.1016/j.epsl.2010.12.050

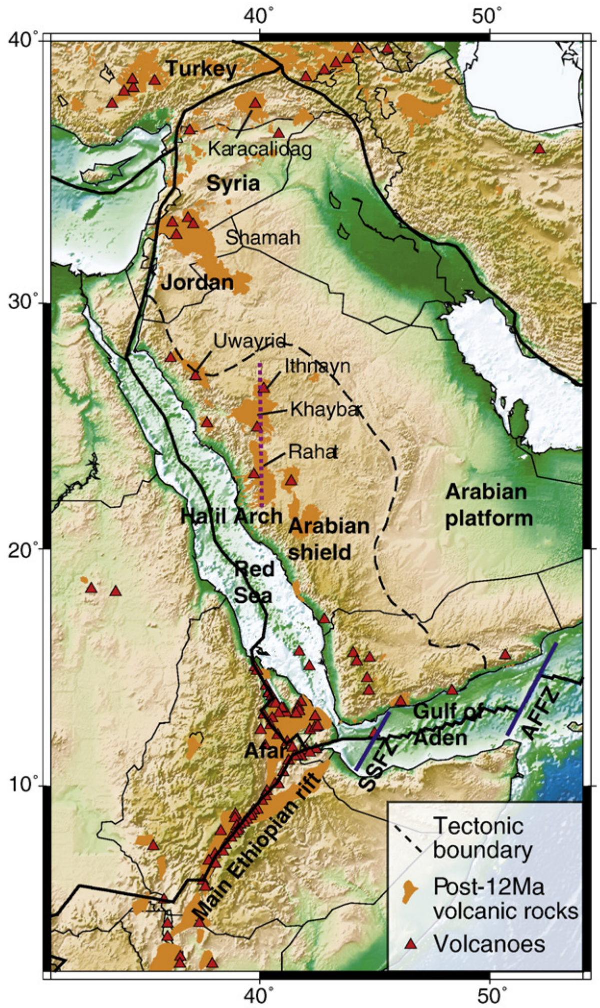

Fig. 1. Topographic map for Arabia and northeastern Africa. Volcanoes and post-12 Ma volcanic rocks are indicated by red triangles and orange area, respectively. Thick solid lines indicate plate boundaries, which are from Bird (2003). A dotted purple line represents the Ha'il Arch. SSFZ: Shukra El Sheik Fracture zone; AFFZ: Alula Fartak Fracture zone.

channel? Can the Afar plume exploit such a channel to cause volcanism as far as Jordan and Turkey? To answer these questions, we jointly invert teleseismic *S*- and *SKS*-arrival times, regional *S*- and Rayleigh waveform fits, fundamental-mode Rayleigh-wave group velocities, and independent Moho constraints to provide complementary resolution for the three-dimensional (3-D) *S*-velocity structure beneath East Africa and Arabia. We demonstrate the unprecedented resolving power of these combined data sets through a series of tests. Our tomographic results help reconcile some of the aforementioned contradictory explanations for the region's volcanism, uplift, and rifting.

2. Method and data

Details on the method and data are given in Chang et al. (2010), but we briefly review them here. Model parameters of *S* velocity are at nodes in a spherical shell at each of 32 different depths, down to 1930 km. The 33rd spherical shell contains model parameters of Moho depth. The shells extend 70° in all directions from the center of our region (35°N/22.5°E). Each spherical shell includes 16,541 nodes roughly 100 km apart at the Earth's surface.

The equation of the joint inversion is as follows

$$\begin{bmatrix} w_{ta}\mathbf{A^{ta}} & w_{ta}\mathbf{A^{ta}_m} & w_{ta}\mathbf{A^{ta}_e} & w_{ta}\mathbf{A^{ta}_o} \\ w_{rw}\mathbf{A^{rw}} & w_{rw}\mathbf{A^{rw}_m} & 0 & 0 \\ w_U\mathbf{A^U} & w_U\mathbf{A^U_m} & 0 & 0 \\ 0 & w_{ic}\mathbf{A^{ic}_m} & 0 & 0 \\ w_1\mathbf{I} & w_1\mathbf{I} & 0 & 0 \\ w_2\mathbf{F_h} & w_2\mathbf{F_h} & 0 & 0 \\ w_3\mathbf{F_v} & 0 & 0 & 0 \end{bmatrix} \begin{bmatrix} \Delta\beta \\ \Delta h \\ \Delta x_e \\ \Delta e \end{bmatrix} = \begin{bmatrix} w_{ta}d^{ta} \\ w_{rw}d^{rw} \\ w_U d^U \\ w_{ic}d^{ic} \\ 0 \\ 0 \\ 0 \end{bmatrix}, \quad (1)$$

where $\mathbf{A^{ta}}$, $\mathbf{A^{rw}}$, $\mathbf{A^U}$, and $\mathbf{A^{ic}}$ are sensitivity matrices to *S* velocity of teleseismic arrival times, regional waveform fits, Rayleigh-wave group velocities, and independent Moho constraints, respectively. The corresponding data vectors are d^{ta}, d^{rw}, d^U, and d^{ic}, respectively. The sensitivity kernels of each data type to Moho depth are represented as $\mathbf{A^{ta}_m}$, $\mathbf{A^{rw}_m}$, $\mathbf{A^U_m}$, and $\mathbf{A}^{ic}_m$, respectively, and the sensitivity kernels to the event location and origin time for teleseismic arrival times are indicated by $\mathbf{A^{ta}_e}$ and $\mathbf{A^{ta}_o}$, respectively. One of several different 1-D reference models is chosen for each path of regional waveforms fits and fundamental-mode group velocities based on average Moho depth and ocean depth for the great-circle path to compute more accurate sensitivity kernels. Model parameters consist of $\Delta\beta$, Δh, Δx_e, and Δe, which are perturbations of *S* velocity, Moho depth, events location, and origin time, respectively. The identity matrix $\mathbf{I}$ serves as the damping operator; $\mathbf{F_h}$ and $\mathbf{F_v}$ are horizontal and vertical flattening operators, respectively. Weights w are applied to each data set and operator. The damping operator tends to suppress the effects of data outliers, while the flattening operators avoid rapid non-physical variations of model parameters. Flattening operators are differentials between two laterally or vertically contiguous nodes (Constable et al., 1987; VanDecar, 1991).

Out of a total of about 5600 waveform fits used in the joint inversion, over 3000 waveforms sample the area of interest (Fig. S1a). The frequency content of the waveform fits is generally within the range between 0.006 and 0.1 Hz. Out of all fundamental-mode Rayleigh-wave group-velocity dispersion curves with a period band ranging from 7 to 100 s in the joint inversion, over 5000 dispersion curves sample the study region (Fig. S1b). For relative arrival times, about 3500 teleseismic *S* and 1400 *SKS* phase arrival times are recorded in the study region (Fig. S1c), which are measured with the multi-channel cross-correlation method (VanDecar and Crosson, 1990). We obtained over 40,000 *S* phase arrival times for the study region (Fig. S1c) from the reprocessed ISC database (Engdahl et al., 1998). We incorporated around 400 Moho depth constraints from receiver functions, gravity measurements, refraction, and reflection surveys (Chang et al., 2010; Marone et al., 2003) to avoid mapping crustal structure into mantle structure (Fig. S1d).

3. Resolution tests

We performed several resolution tests to investigate the resolving power of the joint inversion for the study region. First, we test models with vertical cylindrical anomalies of ±200 m/s, but with different radii of 3° and 1°, as shown in the top panels of Fig. S2. Gaussian random noise is added to synthetic data for the inversion with a standard deviation in proportion to the estimated uncertainty of our data. The cylindrical anomalies with radii of 3° are well resolved beneath Arabia and Ethiopia down to the lower mantle with good amplitude recovery (Fig. S2a). The western boundary of the study region and the Arabian Sea have limited resolution for the whole mantle, but these regions are not of interest in the present paper. Small anomalies with radii of 1° are recovered fairly, with weaker amplitude and some smearing (Fig. S2b), but it is encouraging that anomalies with radii of as small as 1° can be consistently resolved down to 1400 km depth beneath Arabia and Ethiopia.

To test the ability to resolve vertical variations in *S* velocity, we performed checkerboard resolution tests, shown in Fig. S3. Below line A-a through Ethiopia and southern Arabia, anomalies are well recovered for the upper mantle, but resolved with limitation in the lower mantle. For lines B-b and C-c traversing Arabia, the resolution is fair for the lower mantle and better for the upper mantle. These tests show that relatively small or narrow features beneath Arabia from the joint inversion are resolved throughout the mantle.

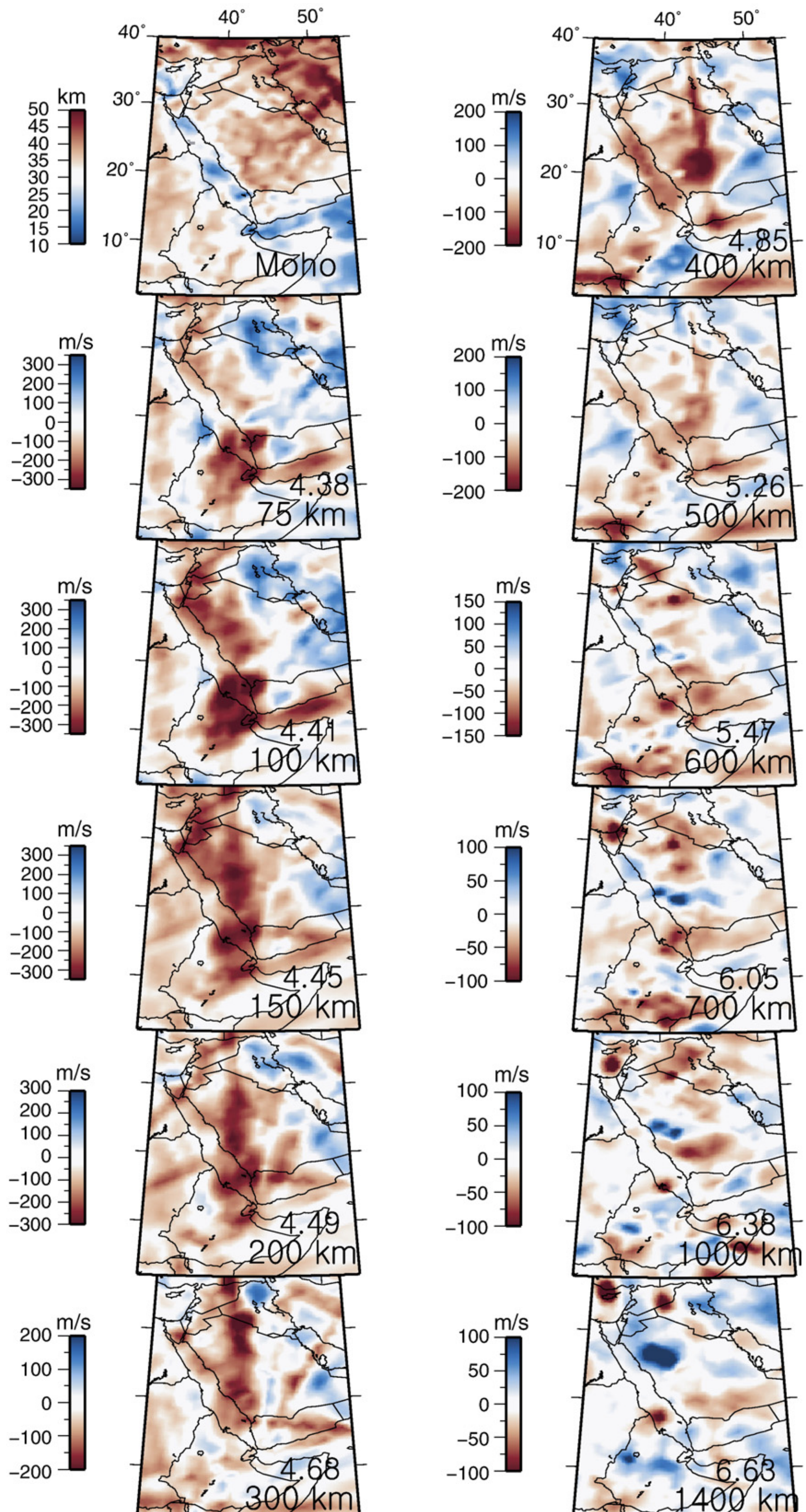

Fig. 2. Moho depth distribution and depth slices at 75, 100, 150, 200, 300, 400, 500, 600, 700, 1000, and 1400 km from the joint inversion model. Velocity perturbations are relative to the reference model "MEAN" (Marone et al., 2004), and the reference *S* velocity at each depth is written on the right side in km/s scale.

4. Results

The Moho depth distribution and depth slices of the joint inversion results are shown in Fig. 2. At 75–100 km depth, a very low velocity anomaly is found beneath Afar and is most likely related to the Cenozoic volcanism around Afar. This volcanism was so extensive that Hofmann et al. (1997) linked it to global climate change. An elongated low-velocity anomaly is detected underneath the Arabian shield in western Arabia. This anomaly has been interpreted by Daradich et al. (2003) as a thermal upwelling and the cause of dynamic topography for the high-altitude region of Afar and the Arabian shield. We also found a well-confined, elongated low-velocity anomaly at 75–150 km beneath the thin crust of the Gulf of Aden. It appears that a similar low-velocity anomaly does not exist beneath the central Red Sea.

At 150–300 km depth the low-velocity anomaly beneath Afar becomes weaker and a low-velocity channel seems to trend northwards beneath Arabia from Afar. In the same depth range we find a low-velocity anomaly beneath Jordan and Syria, which seems to be discontinuous or only faintly continuous with the northward low-velocity channel beneath Arabia. This low-velocity anomaly seems to extend to southern Turkey, where post-12 Ma volcanism has been documented at Harrat Karacalidag (Fig. 1) and is aligned with the Dead Sea Transform fault. The isolation of this low-velocity anomaly from the Afar low-velocity anomaly is more apparent below 600 km depth.

Cross sections through the joint tomographic model are presented in Fig. 3. The upper mantle and the transition zone are dominated by low-velocity anomalies beneath a broad region including the East African rift, the Main Ethiopian rift (MER), Afar, and western Arabia, consistent with previous tomographic results (Bastow et al., 2008; Benoit et al., 2006a,b; Debayle et al., 2001; Park et al., 2007, 2008; Sicilia et al., 2008). Beneath line A-a two narrow low-velocity anomalies, one beneath northern Kenya and the other beneath southern Red Sea (Afar), could represent upwellings from the lower mantle (~1400 km) to the surface, which are also shown in depth slice maps (Fig. 2). Although the resolution test for line A-a (Fig. S3) shows limited checker resolution in the lower mantle, the resolution increases for larger, vertically continuous anomalies, as shown in Fig. S4. Therefore, the low-velocity anomaly beneath northern Kenya, although affected by smearing, may represent a substantial volume of relatively hot mantle. We do not know to which extent this low-velocity anomaly extends southwards because of diminishing resolution to the south.

Beneath line B-b (Fig. 3), we observe two low-velocity anomalies that extend throughout the lower mantle beneath northern and southern Arabia, respectively. These two anomalies are well resolved (Figs. S3 and S4) and could represent mantle plumes. The former low-velocity anomaly beneath northern Arabia and Jordan is also shown in cross section C-c (Fig. 3), for which resolution tests (Figs. S3 and S4)

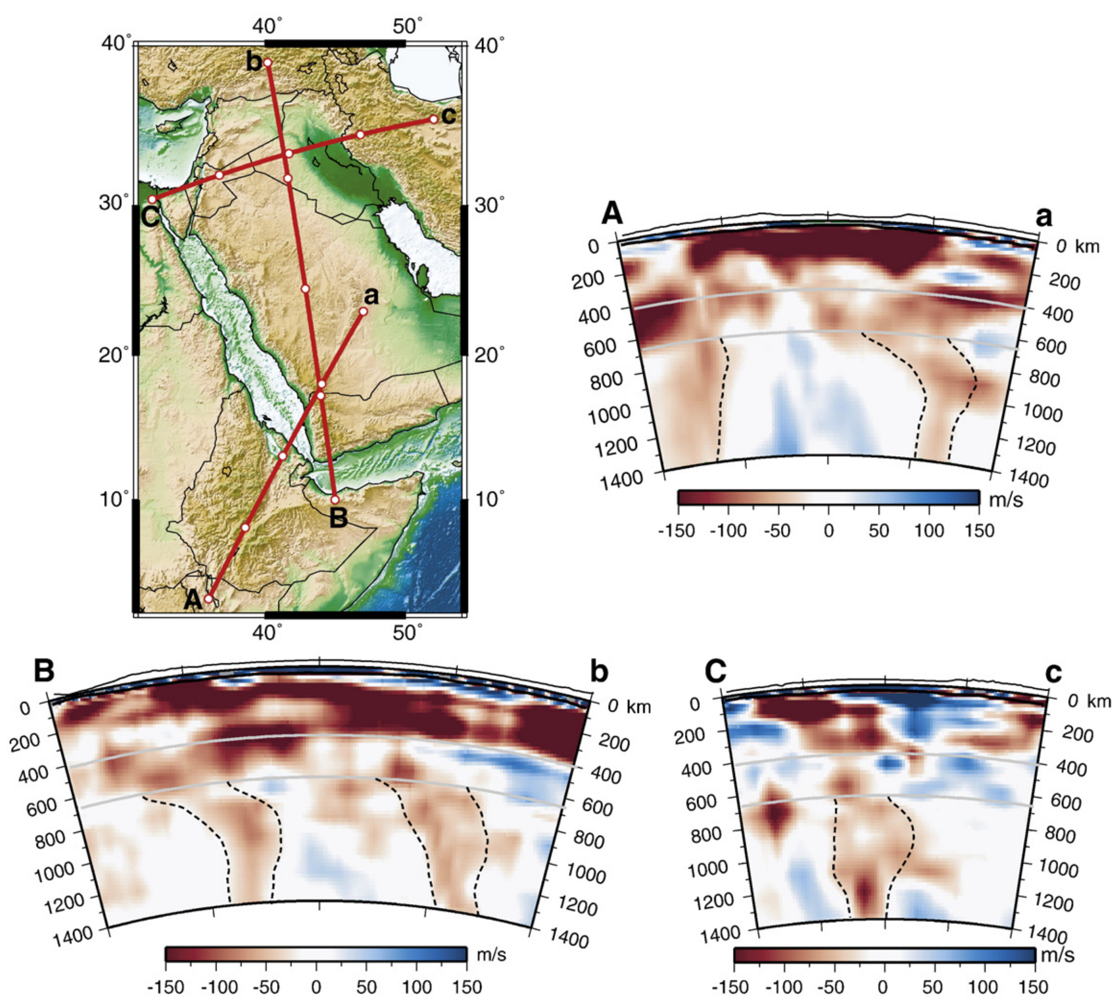

Fig. 3. Vertical cross-section maps encompassing Ethiopia and southern Arabia (A-a), across the Arabian Peninsula in approximately NS direction (B-b), and from the Sinai Peninsula to Iran (C-c). Low-velocity anomalies, which are thought to be mantle plumes, are surrounded by dashed lines. Moho depth and 10 times exaggerated surface topography are indicated by black lines. Gray lines represent discontinuities at 410 and 660 km. Great-circle paths corresponding to cross sections are shown on the left-top map. White circles on the great-circle paths correspond to ticks in the cross sections.

confirm that this anomaly is well resolved throughout the mantle, suggesting a separate plume beneath this region.

5. Discussion

5.1. How many plumes exist with different origins beneath East Africa and Arabia?

The geochemical and geophysical communities appear to disagree in regard to the number of plumes beneath East Africa. Some geochemical research concludes that there are two distinct plumes beneath Afar and Kenya (George et al., 1998; Nelson et al., 2007, 2008; Pik et al., 2006; Rogers et al., 2000), while the single large plume hypothesis is strong in the geophysical community (Daradich et al., 2003; Ebinger and Sleep, 1998; Ritsema et al., 1999).

With the unprecedented resolution obtained from the joint seismic tomography, we provide additional, new clues to this debate. Through the joint inversion, we have imaged two separate quasi-vertical low-velocity anomalies beneath East Africa with different origins down to the lower mantle. One explanation for these anomalies is that both represent mantle plumes. One of these two plumes is located beneath Kenya, the southern margin of our study area. Diminishing resolving power at this edge of our study area precludes us from estimating either the diameter or center of a possible Kenya plume. The other of these two plumes is located beneath Afar. This plume's northeastward tilt with increasing depth suggests that the Afar mantle plume does not originate from the African superplume, which is located in opposite direction (Ritsema et al., 1999). Instead, the African superplume could be feeding the Kenya plume.

In addition, we have presented evidence for a separate mantle plume beneath northern Arabia and Jordan. This plume may clarify the simultaneous northward and southward migration of the Neogene volcanism between Afar and Jordan (Bosworth et al., 2005; Camp and Roobol, 1992). The northward migration began on southern Harrat Rahat at about 10 Ma, on Harrat Khaybar at about 5 Ma, and on Harrat Ithnayn at about 3 Ma (Camp and Roobol, 1992; Fig. 1) and the southward migration of the volcanism began on Harrat Shamah at about 13 Ma, on Harrats Uwayrid at around 12 Ma, on Harrat Khaybar at around 11 Ma, and on Harrat Rahat at around 10 Ma (Bosworth et al., 2005). Although Bosworth et al. (2005) and Camp and Roobol (1992) disagree about the age of Harrat Khaybar volcanism, the youngest documented volcanism at Harrat Ithnayn is flanked in both directions by older volcanisms. Furthermore, the notion of a separate mantle plume beneath northern Arabia and Jordan is supported by Harrat Shamah in Jordan having the geochemical signature of a deep origin (Ilani et al., 2001). We suggest here that southward horizontal mantle flow from the plume beneath Jordan and northern Arabia combined with northward mantle flow from the Afar plume may be responsible for the distribution of widespread volcanism, uplift, and rifting in western Arabia (Fig. 1).

5.2. Comparison of our results with shear-wave splitting in East Africa and Arabia

In Fig. 4, we compare locations of the observed three mantle plumes beneath East Africa and Arabia with directions of fast axes of shear-wave splitting in this area (Gashawbeza et al., 2004; Hansen et al., 2006; Walker et al., 2004). Because of limited resolution at the southern edge of our study region, the location of the Kenya plume in Fig. 4 is based on Lin et al. (2005) and Weeraratne et al. (2003). The shear-wave splitting around Afar (Gashawbeza et al., 2004; Hansen et al., 2006) shows large splitting times with NS and SW–NE directions of fast axes beneath Arabia and Ethiopia, respectively. The location of the Afar plume, based on our tomographic results, is consistent with the point where these fast axes abruptly change direction. Therefore, this observation may suggest that the dominant reason for the fast axes is horizontal mantle flow radially away from Afar.

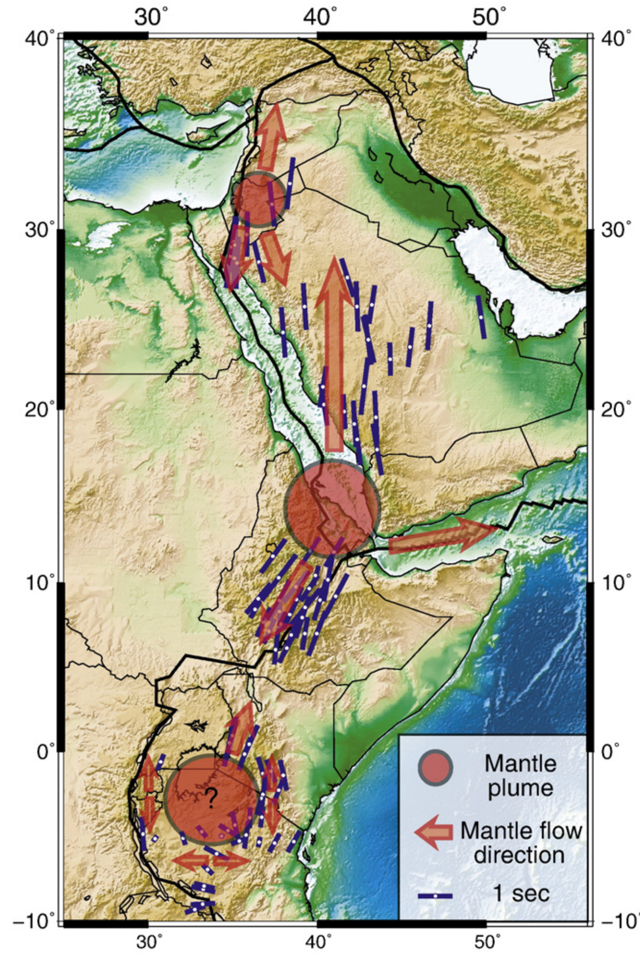

Fig. 4. Schematic map which shows locations of mantle plumes and mantle flow directions along with fast axes of shear-wave splitting. The shear-wave splitting data are obtained from Gashawbeza et al. (2004), Hansen et al. (2006), and Walker et al. (2004). The locations of the Afar and Jordan plumes are from the 150 km depth slice in Fig. 2. The location of the Kenya plume is based on Weeraratne et al. (2003).

Kendall et al. (2005) argue for melt-assisted rifting based on small-scale variations of shear-wave splitting around the MER, but Bastow et al. (2010) and Kendall et al. (2006) do not rule out a contribution from horizontal mantle flow in light of surface-wave tomographic results from Debayle et al. (2005). Moreover, the results in Kendall et al. (2005) may be consistent with hot mantle flowing horizontally from Afar, because the splitting times along the rift decrease with distance from Afar to southern Ethiopia, which implies that the thickness of the flow layer or the degree of strain may be decreasing in this direction. Therefore, an alternative explanation of their observations is that horizontal mantle flow from Afar along the rift is a dominant reason for anisotropy and melts within the rift may alter the direction of fast axes of shear-wave splitting locally.

Further south, Walker et al. (2004) found a similar direction of fast axes of shear-wave splitting north of the possible Kenya plume, whose presumed location coincides with the Tanzanian craton. In addition, they observed small splitting times with concentric fast-axis directions around this location. This pattern along with the larger splitting times around the boundary of the craton compared to those on the craton, agree with results from numerical simulations of a plume beneath a craton (Sleep et al., 2002). It again appears that horizontal mantle flow is the dominant reason for the observed shear-wave splitting (Walker et al., 2004).

Finally, the location of the plume beneath Jordan and northern Arabia may also be a center from which hot mantle material flows horizontally. Such flow is consistent with the fast-axis directions of observed shear-wave splitting (Fig. 4; Hansen et al., 2006). It is possible that similar horizontal mantle flow occurs along the Dead Sea transform fault (Hansen et al., 2006). Therefore, both the Neogene volcanism around Jordan, such as Harrat Shamah and Uwayrid, as well as volcanism at Harrat Karacalidag in southern Turkey may be related to this plume. The latter was reported to have a deep mantle source, similar to ocean island basalts (Sen et al., 2004).

5.3. Do hot materials from Afar flow along thin lithosphere beneath the Red Sea and the Gulf of Aden as a natural channel?

Based on the Cenozoic volcanism along the Red Sea, previous research has argued that the Red Sea is underlain by hot mantle (e.g., Coleman and McGuire, 1988; Dixon et al., 1989). Ebinger and Sleep (1998) proposed rifts may present natural channels for hot material from mantle plumes to flow horizontally beneath thin lithosphere. The Red Sea has been proposed as such a channel for hot material from the Afar plume to cause the Cenozoic volcanism in western Arabia (e.g., Hansen et al., 2006; Park et al., 2007, 2008; Ritsema et al., 1999). However, this hypothesis is inconsistent with the pattern of seismicity and oceanic basalts in the Red Sea. Seismicity is absent beneath the central Red Sea, although high seismicity is observed in the southern Red Sea (Reilinger et al., 2006). There is more oceanic crust in southern Red Sea and less in the central Red Sea (Camp and Roobol, 1992). Moreover, the oceanic basalts in the southern Red Sea has plume signature, whereas the oceanic basalts in the central Red Sea has MORB signature (Barrat et al., 1990; Volker et al., 1997).

Rifting of the Gulf of Aden began around 35 Ma ago, and seafloor spreading has propagated westward from the eastern Gulf of Aden since around 18 Ma ago (Leroy et al., 2004). Some argue that the influence of the Afar mantle plume on the Gulf of Aden ends at the Shukra El Sheik Fracture zone (SSFZ, Fig. 1; Hébert et al., 2001). However, the high heat flow and volcanic activity 1000 km east of Afar reported by Lucazeau et al. (2009) as well as off-axis volcanic structures east of the Alula Fartak fracture zone (AFFZ; Fig. 1) reported by Leroy et al. (2010) suggest that Afar plume material might reach farther east than the SSFZ.

Beneath the Gulf of Aden our tomographic results show a low-velocity anomaly at 75–150 km depth that aligns well with the Gulf of Aden (Fig. 2), supporting the channeled eastward flow from Afar as proposed by Leroy et al. (2010). A very low-velocity anomaly (−7%) is observed at 100 km depth just west of AFFZ, implying the existence of melts.

However, a channel-shaped low-velocity anomaly extending northwards from Afar does not align well with the Red Sea. While this anomaly underlies the southern Red Sea, it continues northwards beneath Arabia leaving the central Red Sea without underlying hot mantle. This is unexpected because thin lithosphere beneath the Red Sea might play a role as a natural channel for the mantle flow as in the case of the Gulf of Aden. Currently available maps of the lithosphere–asthenosphere boundary (LAB) do not have high resolution for this region to map possible natural channels (e.g., Rychert and Shearer 2009; Tkalčić et al., 2006). However, the Ha'il Arch (Fig. 1), which was formed in pre-Permian time and deformed in Late Cretaceous (Bosworth et al., 2005; Coleman, 1974), may present such a natural lithospheric channel and aligns with the imaged long low-velocity anomaly beneath Arabia.

Furthermore, the absolute Arabian plate motion has a direction of ~N45°E in the Indo-Atlantic hotspot reference frame (DeMets et al., 1994; O'Neill et al., 2005; Schellart et al., 2008), and GPS-based measurements also yield a similar direction (ArRajehi et al., 2010). This direction is parallel to the Gulf of Aden, but nearly perpendicular to the Red Sea. Therefore, if original channeled mantle flow from Afar was aligned in the direction of the current Red Sea, the channeled direction might have changed clockwise while trapped under thin lithosphere due to the northeast direction of the Arabian plate motion (Chang, et al., in press). This deflection of the mantle flow due to the influence of a plate motion is also found in the parabolic pattern of mantle flow around the location of a plume (e.g., Walker et al., 2001; Walker et al., 2007). We could explain the difference in seismicity and oceanic crust between the central and southern Red Sea with the deflection of mantle flow from Afar.

6. Conclusions

We estimated a 3-D *S*-velocity structure around Arabia and East Africa down to 1400 km depth by jointly inverting teleseismic *S*- and *SKS*-arrival times, regional waveform fits, Rayleigh-wave group velocities, and independent Moho constraints from receiver functions, refraction/reflection profiles, and gravity surveys. This method provides more comprehensive resolution than previous studies based on subsets of these data (Chang et al., 2010).

Two distinct low-velocity anomalies, likely representing mantle plumes, are found beneath Afar and northern Kenya, which extend down to at least 1400 km depth. However, we could not resolve the southern extent of the Kenya plume. Extensive low-velocity anomalies in the uppermost mantle along with the shear-wave splitting results suggest horizontal mantle flow radially away from Afar. This radial flow seems to be organized in channels, potentially following thin lithosphere. One such channel follows the Gulf of Aden, supporting the notion of eastward channeled mantle flow from Afar. Another channel extends northward beneath the southern Red Sea, but rather than extending to the central Red Sea, it continues northwards beneath Arabia.

A separate quasi-vertical low-velocity anomaly is found beneath Jordan and northern Arabia, likely representing a separate plume that may be responsible for Harrat Shamah in Jordan and Harrat Uwayrid in northern Arabia. This low-velocity anomaly extends significantly into the lower mantle, supporting geochemical evidence (Ilani et al., 2001) that the Neogene volcanism in Jordan has a deep mantle origin. This mantle plume may have contributed, along with the Afar plume, to the widespread volcanism and uplift in western Arabia.

Acknowledgments

We thank Dr. Yongcheol Park for providing digital data for locations of volcanoes and post-12 Ma volcanic rocks and for sharing his relative arrival times. We also thank three anonymous reviewers whose comments greatly improved this manuscript. All figures were created using Generic Mapping Tools (GMT; Wessel and Smith, 1998). This work was supported by the Korea Research Foundation Grant KRF-2006-214-C00092 funded by the Korean Government (MOEHRD), the U.S. DOE under contract DE-FC52-04NA25541, and Northwestern University.

Appendix A. Supplementary data

Supplementary data to this article can be found online at doi:10.1016/j.epsl.2010.12.050.

References

ArRajehi, A., et al., 2010. Geodetic constraints on present-day motion of the Arabian plate: implications for Red Sea and Gulf of Aden rifting. Tectonics 29, TC3011. doi:10.1029/2009TC002482.

Barrat, J.-A., Jahn, B.M., Joron, J.-L., Auvray, B., Hamdi, H., 1990. Mantle heterogeneity in northeastern Africa: evidence from Nd isotopic compositions and hygromagmaphile element geochemistry of basaltic rocks from the Gulf of Tadjoura and southern Red Sea regions. Earth Planet. Sci. Lett. 101, 233–247.

Bastow, I.D., Nyblade, A.A., Stuart, G.W., Rooney, T.O., Benoit, M.H., 2008. Upper mantle seismic structure beneath the Ethiopian hot spot: rifting at the edge of the African low-velocity anomaly. Geochem. Geophys. Geosyst. 9, Q12022. doi:10.1029/2008GC002107.

Bastow, I.D., Pilidou, S., Kendall, J.-M., Stuart, G.W., 2010. Melt-induced seismic anisotropy and magma assisted rifting in Ethiopia: evidence from surface waves. Geochem. Geophys. Geosyst. 11, Q0AB05. doi:10.1029/2010GC003036.

Benoit, M.H., Nyblade, A.A., VanDecar, J.C., 2006a. Upper mantle P-wave speed variations beneath Ethiopia and the origin of the Afar hotspot. Geology 34, 329–332.

Benoit, M.H., Nyblade, A.A., Owens, T.J., Stuart, G., 2006b. Mantle transition zone structure and upper mantle S velocity variations beneath Ethiopia: evidence for a broad, deep-seated thermal anomaly. Geochem. Geophys. Geosyst. 7, Q11013. doi:10.1029/2006GC001398.

Bird, P., 2003. An updated digital model of plate boundaries. Geochem. Geophys. Geosyst. 4, 1027. doi:10.1029/2001GC000252.

Bosworth, W., Huchon, P., McClay, K., 2005. The Red Sea and Gulf of Aden Basins. J. African Earth Sci. 43, 334–378.

Camp, V.E., Roobol, M.J., 1992. Upwelling asthenosphere beneath western Arabia and its regional implications. J. Geophys. Res. 97, 15255–15271.

Chang, S.-J., Merino, M., van der Lee, S., Stein, S., Stein, C., in press, Mantle flow beneath Arabia offset from the opening Red Sea. Geophys. Res. Lett.

Chang, S.-J., van der Lee, S., Flanagan, M.P., Bedle, H., Marone, F., Matzel, E.M., Pasyanos, M.E., Rodgers, A.J., Romanowicz, B., Schmid, C., 2010. Joint inversion for 3-dimenstional S-velocity mantle structure along the Tethyan margin. J. Geophys. Res. 115, B08309. doi:10.1029/2009JB007204.

Coleman, R.G., 1974. Geologic background of the Red Sea. In: Burk, C.A., Drake, D.L. (Eds.), The Geology of Continental Margins. Springer-Verlag, New York, pp. 743–751.

Coleman, R.G., McGuire, A.V., 1988. Magma systems related to the Red Sea opening. Tectonophysics 150, 77–100.

Constable, S.C., Parker, R.L., Constable, C.G., 1987. Occam's inversion: a practical algorithm for generating smooth models from electromagnetic sounding data. Geophysics 52, 289–300.

Daradich, A., Mitrovica, J.X., Pysklywec, R.N., Willett, S.D., Forte, A.M., 2003. Mantle flow, dynamic topography, and rift-flank uplift of Arabia. Geology 31, 901–904.

Debayle, E., Kennett, B.L.N., Priestley, K., 2005. Global azimuthal seismic anisotropy and the unique plate-motion deformation of Australia. Nature 433, 509–512.

Debayle, E., Lévêque, J.J., Cara, M., 2001. Seismic evidence for a deeply rooted low-velocity anomaly in the upper mantle beneath the northeastern Afro/Arabian continent. Earth Planet. Sci. Lett. 193, 423–436.

DeMets, C., Gordon, R.G., Argus, D.F., Stein, S., 1994. Effect of recent revisions to the geomagnetic reversal time scale on estimates of current plate motions. Geophys. Res. Lett. 21, 2191–2194.

Dixon, T.H., Ivins, E.R., Franklin, B.J., 1989. Topographic and volcanic asymmetry around the Red Sea: constraints on rift models. Tectonics 8, 1193–1216.

Ebinger, C.J., Sleep, N.H., 1998. Cenozoic magmatism throughout east Africa resulting from impact of a single plume. Nature 395, 788–791.

Engdahl, E.R., van der Hilst, R., Buland, R., 1998. Global teleseismic earthquake relocation with improved travel times and procedures for depth determination. Bull. Seism. Soc. Am. 88, 722–743.

Furman, T., Bryce, J., Rooney, T., Hanan, B., Yirgu, G., Ayalew, D., 2006. Heads and tails: 30 million years of the Afar plume. In: Yirgu, G., Ebinger, C., Maguire, P.K.H. (Eds.), The Afar volcanic province within the East African Rift System: Geol. Soc. Spec. Publ., 259, pp. 95–119.

Gashawbeza, E.M., Klemperer, S.L., Nyblade, A.A., Walker, K.T., Keranen, K.M., 2004. Shear-wave splitting in Ethiopia: Precambrian mantle anisotropy locally modified by Neogene rifting. Geophys. Res. Lett. 31, L18602. doi:10.1029/2004GL020471.

George, R., Rogers, N., Kelley, S., 1998. Earliest magmatism in Ethiopia: evidence for two mantle plumes in one flood basalt province. Geology 26, 923–926.

Hansen, S., Schwartz, S., Al-Amri, A., Rodgers, A., 2006. Combined plate motion and density-driven flow in the asthenosphere beneath Saudi Arabia: evidence from shear-wave splitting and seismic anisotropy. Geology 34, 869–872. doi:10.1130/G22713.1.

Hébert, H., Deplus, C., Huchon, P., Khanbari, K., Audin, L., 2001. Lithospheric structure of a nascent spreading ridge inferred from gravity data: the western Gulf of Aden. J. Geophys. Res. 106, 26,345–26,363.

Hofmann, C., Courtillot, V., Féraud, G., Rochette, P., Yirgu, G., Ketefo, E., Pik, R., 1997. Timing of the Ethiopian flood basalt event and implications for plume birth and global change. Nature 389, 838–841.

Ilani, S., Harlavan, Y., Tarawneh, K., Rabba, I., Weinberger, R., Ibrahim, K., Peltz, S., Steinitz, G., 2001. New K-Ar ages of basalts from the Harrat Ash Shaam volcanic field in Jordan: implications for the span and duration of the upper-mantle upwelling beneath the western Arabian plate. Geology 29, 171–174.

Kendall, J.-M., Pilidou, S., Keir, D., Bastow, I.D., Stuart, G.W., Ayele, A., 2006. Mantle upwellings, melt migration and the rifting of Africa: insights from seismic anisotropy. In: Yirgu, G., Ebinger, C., Maguire, P.K.H. (Eds.), The Afar volcanic province within the East African Rift System: Geol. Soc. Spec. Publ., 259, pp. 55–72.

Kendall, J.-M., Stuart, G.W., Ebinger, C.J., Bastow, I.D., Keir, D., 2005. Magma-assisted rifting in Ethiopia. Nature 433, 146–148.

Leroy, S., d'Acremont, E., Tiberi, C., Basuyau, C., Autin, J., Lucazeau, F., Sloan, H., 2010. Recent off-axis volcanism in the eastern Gulf of Aden: implications for plume–ridge interaction. Earth Planet. Sci. Lett. 293, 140–153.

Leroy, S., Gente, P., Fournier, M., d'Acremont, E., Patriat, P., Beslier, M.-O., Bellahsen, N., Maia, M., Blais, A., Perrot, J., Al-Kathiri, A., Merkouriev, S., Fleury, J.-M., Ruellan, P.-Y., Lepvrier, C., Huchon, P., 2004. From rifting to spreading in the eastern Gulf of Aden: a geophysical survey of a young oceanic basin from margin to margin. Terra Nova 16, 185–192.

Lin, S.-C., Kuo, B.-Y., Chiao, L.-Y., van Keken, P.E., 2005. Thermal plume models and melt generation in East Africa: a dynamic modeling approach. Earth Planet. Sci. Lett. 237, 175–192.

Lucazeau, F., Leroy, S., Autin, J., Bonneville, A., Goutorbe, B., Watremez, L., d'Acremont, E., Düsünur, D., Rolandone, F., Huchon, P., Bellahsen, N., Tuchais, P., 2009. Post-rift volcanism and high heat-flow at the ocean-continent transition of the eastern Gulf of Aden. Terra Nova 21, 285–292.

Marone, F., van der Lee, S., Giardini, D., 2004. Three-dimensional upper-mantle S-velocity model for the Eurasia–Africa plate boundary region. Geophys. J. Int. 158, 109–130.

Marone, F., van der Meijde, M., van der Lee, S., Giardini, D., 2003. Joint inversion of local, regional and teleseismic data for crustal thickness in the Eurasia–Africa plate boundary region. Geophys. J. Int. 154, 499–514.

Montelli, R., Nolet, G., Dahlen, F.A., Masters, G., 2006. A catalogue of deep mantle plumes: new results from finite-frequency tomography. Geochem. Geophys. Geosyst. 7, Q11007. doi:10.1029/2006GC001248.

Montelli, R., Nolet, G., Dahlen, F.A., Masters, G., Engdahl, E.R., Hung, S.-H., 2004. Finite-frequency tomography reveals a variety of plumes in the mantle. Science 303, 338–343.

Nelson, W.R., Furman, T., van Keken, P.E., Lin, S., 2007. Two plumes beneath the East African Rift System: a geochemical investigation into possible interactions in Ethiopia. Eos. Trans. AGU 88 (52) Fall Meet. Suppl., Abstract V42B-04.

Nelson, W.R., Furman, T., Hanan, B., 2008. Sr, Nd, Pb and Hf evidence for two-plume mixing beneath the East African Rift System. Geochim. Cosmochim. Acta 72, A676.

O'Neill, C., Müller, D., Steinberger, B., 2005. On the uncertainties in hot spot reconstructions and the significance of moving hot spot reference frames. Geochem. Geophys. Geosyst. 6, Q04003. doi:10.1029/2004GC000784.

Park, Y., Nyblade, A.A., Rodgers, A.J., Al-Amri, A., 2007. Upper mantle structure beneath the Arabian Peninsula and northern Red Sea from teleseismic body wave tomography: implication for the origin of Cenozoic uplift and volcanism in the Arabian Shield. Geochem. Geophys. Geosyst. 8, Q06021. doi:10.1029/2006GC001566.

Park, Y., Nyblade, A.A., Rodgers, A.J., Al-Amri, A., 2008. S wave velocity structure of the Arabian Shield upper mantle from Rayleigh wave tomography. Geochem. Geophys. Geosyst. 9, Q07020. doi:10.1029/2007GC001895.

Pik, R., Marty, B., Hilton, D.R., 2006. How many mantle plumes in Africa? The geochemical point of view. Chem. Geol. 226, 100–114.

Reilinger, R., McClusky, S., Vernant, P., Lawrence, S., Ergintav, S., Cakmak, R., Ozener, H., Kadirov, F., Guliev, I., Stepanyan, R., Nadariya, M., Hahubia, G., Mahmoud, S., Sakr, K., ArRajehi, A., Paradissis, D., Al-Aydrus, A., Prilepin, M., Guseva, T., Evren, E., Dmitrotsa, A., Filikov, S.V., Gomez, F., Al-Ghazzi, R., Karam, G., 2006. GPS constraints on continental deformation in the Africa–Arabia–Eurasia continental collision zone and implications for the dynamics of plate interactions. J. Geophys. Res. 111, B05411. doi:10.1029/2005JB004051.

Ritsema, J., van Heijst, H.J., Woodhouse, J.H., 1999. Complex shear wave velocity structure imaged beneath Africa and Iceland. Science 286, 1925–1928.

Rogers, N., Macdonald, R., Fitton, J.G., George, R., Smith, M., Barreiro, B., 2000. Two mantle plumes beneath the East African rift system: Sr, Nd and Pb isotope evidence from Kenya Rift basalts. Earth Planet. Sci. Lett. 176, 387–400.

Rychert, C.A., Shearer, P.M., 2009. A global view of the lithosphere–asthenosphere boundary. Science 324, 495–498.

Schellart, W.P., Stegman, D.R., Freeman, J., 2008. Global trench migration velocities and slab migration induced upper mantle volume fluxes: constraints to find an Earth reference frame based on minimizing viscous dissipation. Earth Sci. Rev. 88, 118–144.

Schilling, J.-G., 1973. Afar mantle plume: rare earth evidence. Nat. Phys. Sci. 242, 2–6.

Sen, P.A., Temel, A., Gourgaud, A., 2004. Petrogenetic modeling of Quaternary post-collisional volcanism: a case study of central and eastern Anatolia. Geol. Mag. 141, 81–98.

Sicilia, D., Montagner, J.-P., Cara, M., Stutzmann, E., Debayle, E., Lepine, J.-C., Leveque, J.-J., Beucler, E., Sebai, A., Roult, G., Ayele, A., Sholan, J.M., 2008. Upper mantle structure of shear-wave velocities and stratification of anisotropy in the Afar Hotspot region. Tectonophysics 462, 164–177.

Sleep, N.H., Ebinger, C.J., Kendall, J.-M., 2002. Deflection of mantle plume material by cratonic keels. In: Fowler, C.M.R., Ebinger, C.J., Hawkesworth, C.J. (Eds.), The Early Earth: Physical, Chemical and Biological Development: Geol. Soc. Spec. Publ., 199, pp. 135–150.

Tkalčić, H., Pasyanos, M.E., Rodgers, A.J., Gök, R., Walter, W.R., Al-Amri, A., 2006. A multistep approach for joint modeling of surface wave dispersion and teleseismic receiver functions: implications for lithospheric structure of the Arabian Peninsula. J. Geophys. Res. 111, B11311. doi:10.1029/2005JB004130.

VanDecar, J.C., 1991. Upper-mantle structure of the Cascadia subduction zone from non-linear teleseismic travel-time inversion. Ph.D. thesis, University of Washington, Seattle.

VanDecar, J.C., Crosson, R.S., 1990. Determination of teleseismic relative phase arrival times using multi-channel cross-correlation and least-squares. Bull. Seism. Soc. Am. 80, 150–169.

Volker, F., Altherr, R., Jochum, K.-P., McCulloch, M.T., 1997. Quaternary volcanic activity of the southern Red Sea: new data and assessment of models on magma sources and Afar plume–lithosphere interaction. Tectonophysics 278, 15–29.

Walker, K.T., Bokelmann, G.H.R., Klemperer, S.L., 2001. Shear-wave splitting to test mantle deformation models around Hawaii. Geophys. Res. Lett. 28, 4319–4322.

Walker, K.T., Bokelmann, G.H.R., Klemperer, S.L., Bock, G., the Eifel Plume Team, 2007. Seismic anisotropy in the asthenosphere beneath the Eifel region, western Germany. In: Ritter, J.R.R., Christensen, U.R. (Eds.), Mantle Plumes: A Multidisciplinary Approach. Springer-Verlag, Berlin, pp. 439–464.

Walker, K.T., Nyblade, A.A., Klemperer, S.L., Bokelmann, G.H.R., Owens, T.J., 2004. On the relationship between extension and anisotropy: constraints from shear wave splitting across the East African Plateau. J. Geophys. Res. 109, B08302. doi:10.1029/2003JB002866.

Weeraratne, D.S., Forsyth, D.W., Fischer, K.M., Nyblade, A.A., 2003. Evidence for an upper mantle plume beneath the Tanzanian craton from Rayleigh wave tomography. J. Geophys. Res. 108, 2427. doi:10.1029/2002JB002273.

Wessel, P., Smith, W.H.F., 1998. New, improved version of the Generic Mapping Tools released. EOS Trans. AGU 79, 579.

White, R.S., McKenzie, D.P., 1989. Magmatism at rift zones: the generation of volcanic continental margins and flood basalts. J. Geophys. Res. 94, 7685–7729.